Physics Letters A 377 (2013) 2388–2392

Contents lists available at SciVerse ScienceDirect

Physics Letters A

www.elsevier.com/locate/pla

A kinetic theory of micromagnetic time evolution

G.J. Parker [a,*], W.N.G. Hitchon [b]

[a] HGST, 3904 Yueba Buena Rd., San Jose, CA 95135, United States

[b] Department of Electrical and Computer Engineering, University of Wisconsin–Madison, Madison, WI 53706, United States

ARTICLE INFO

Article history:
Received 6 December 2012
Received in revised form 6 May 2013
Accepted 20 June 2013
Available online 28 June 2013
Communicated by R. Wu

Keywords:
Micromagnetics
Hysteresis loops
Kinetic theory
Transition rate
Computation for stiff problems

ABSTRACT

A semi-analytic description of recording media grains' magnetization flipping in a magnetic field provides hysteresis loops, efficiently, with all parameters found by following orbits, and in close agreement with existing results. Integrating the Landau–Lifshitz–Gilbert (LLG) equations numerically gives the average energy diffusion coefficient D_ϵ, energy loss rate a_ϵ and the barrier height which must be overcome. These allow solution of the kinetic equation for the probability density f and the escape rate γ of a grain trapped in an energy well, as well as other, similar, very stiff systems. γ is used in Monte Carlo simulation of hysteresis. The essential physics governing the grains' behavior is outlined.

1. Introduction

The simulation of micromagnetic systems is of great technological importance [1–8], including addressing the stability of magnetic recording media and slow hysteresis loops [9–13]. However, the enormous disparity in the relevant timescales makes direct simulations impractical. This study concerns transition rates of grains, (strictly, the magnetic moments of the grains are meant when we speak of grains) escaping due to thermal effects from a local minimum in the energy. As in many physical situations, the fastest processes are close to a relaxed equilibrium. The LLG equation

$$\frac{d\hat{m}}{dt} = -\gamma_0 \hat{m} \times (\vec{H}_{\text{eff}} + \vec{H}_{\text{th}}) + \alpha \hat{m} \times \frac{d\hat{m}}{dt} \tag{1}$$

must be integrated for of order 10^{12} steps in the escape time. In Eq. (1), $\hat{m} = \vec{M}/M_s$, $\vec{M}$ is the macroscopic magnetization with saturation magnetization M_s, γ_0 is the gyromagnetic ratio (1.76×10^7 Oe^{-1} s^{-1}), α is the phenomenological damping (0.1 used here) and the effective field, $\vec{H}_{\text{eff}} \equiv -\partial G(\vec{M}, \vec{H}_{\text{a}})/\partial \vec{M}$, where the micromagnetic free energy $G(\vec{M}, \vec{H}_{\text{a}})$ consists of exchange, uniaxial anisotropy, magnetostatic and Zeeman energies. The Zeeman energy arises from the external applied fields, $\vec{H}_{\text{a}}$. Including W.F. Brown's [9] stochastic "thermal field", $\vec{H}_{\text{th}}$, Eq. (1) results in the Langevin equation [11,12].

In the next section we solve a 'kinetic equation' of the drift–diffusion type for the probability density f of the grains as a function of energy and hence the transition rate γ. In Section 3 the orbit-averaged diffusion coefficient in energy D_ϵ and the energy loss rate a_ϵ are obtained. The barrier height is also found by orbit following. Fluctuations in barrier height observed in orbit following allow a probability distribution of barrier heights to be generated, and from this distribution and the expression for the escape rate γ we obtain a mean barrier height that corresponds to the escape rate averaged over barrier heights. In Section 4, γ is used in a Monte Carlo simulation of a group of grains, generating hysteresis curves which agree closely with curves obtained using the standard approach of Xue & Victora (XV) [13]. XV uses arbitrary parameters constrained by computational limitations and can be much slower than the present micromagnetic kinetic theory (MMKT) technique, which handles problems not previously tractable, such as varying sweep rates during hysteresis loops or simulation of thermal decay of written bit patterns in arbitrary applied fields. Finally, Section 5 is a summary, indicating the essential physics of the system of grains trapped in potential wells. We emphasize orbit-averaged transport coefficients with respect to energy (which simplify the problem, especially near the saddle point in the energy surfaces) and the fluctuation in barrier height which the grains experience.

* Corresponding author. Tel.: +1 408 717 7583; fax: +1 408 717 9065.
E-mail address: gregory.parker@hgst.com (G.J. Parker).

0375-9601
http://dx.doi.org/10.1016/j.physleta.2013.06.030

2. A kinetic equation for the grain

Let $f(\epsilon,t)\,d\epsilon$ be the probability that a single grain in an energy well has energy from ϵ to $\epsilon+d\epsilon$ at time t, $\epsilon \equiv G(\vec{M},\vec{H}_a) - G(\vec{M}_0,\vec{H}_a)$ and $\vec{M}_0$ is the magnetization vector that corresponds to the local minimum energy. If D_ϵ is the energy diffusion coefficient, arising from thermal effects, and $a_\epsilon(>0)$ is the energy loss rate due to damping, then if the density of states is (approximately) constant there is a diffusive flux of probability in energy $\Gamma_{\rm diff} \equiv -D_\epsilon \frac{\partial f}{\partial \epsilon}$, and a drift flux $\Gamma_{\rm drift} \equiv -a_\epsilon f$, so the total flux of probability density in energy is

$$\Gamma = -a_\epsilon f - D_\epsilon \frac{\partial f}{\partial \epsilon}. \tag{2}$$

We emphasize that this approach is a drift–diffusion model, distinct from the Fokker–Planck model [14]. Brown goes to some lengths to show the equivalence of the two approaches [9]. We return to the comparison with Brown's results below. The kinetic equation, which is an equation of conservation of probability, is

$$\frac{\partial f}{\partial t} + \frac{\partial \Gamma}{\partial \epsilon} = 0. \tag{3}$$

Numerical solution can be difficult when the system is close to equilibrium, since $\Gamma_{\rm drift}$ and $\Gamma_{\rm diff}$ cancel to extremely high precision. A semi-analytic solution will be described, in the spirit of Scharfetter and Gummel [15], which builds-in that $\Gamma_{\rm drift}+\Gamma_{\rm diff}$ is small. This guarantees $f(\epsilon)$ converges to the Boltzmann density f_B as the escape probability goes to zero.

We make a number of approximations which may be relaxed in future. First, we approximate D_ϵ and a_ϵ as being constants in each of a large number of regions, i.e. as histograms. Second, we set $f(\epsilon)=0$ at the maximum energy $\epsilon_{\rm max}$ (the saddle point energy, which is the lowest barrier the grain has to overcome between the true energy minima), and we set the flux of probability in energy to zero, $\Gamma(\epsilon)=0$, at zero energy (i.e. at the local minimum). At the boundary between each adjacent pair of regions of constant D_ϵ and a_ϵ we enforce continuity of probability f and probability flux, $\Gamma(\epsilon)$.

We seek a solution in the form

$$f(\epsilon,t) = F(\epsilon)\tau(t) \quad\Rightarrow\quad \tau(t) = \exp(-\gamma t), \tag{4}$$

a separable solution where all the regions have the same rate constant, γ. For each region we assume F varies as $\exp(r\epsilon)$ and using $D_\epsilon/a_\epsilon = kT$ (see below) where T is the temperature, therefore

$$r_{1,2} = -\frac{1}{2kT}\left(1 \pm \sqrt{1-4\gamma kT/a_\epsilon}\right). \tag{5}$$

Then within each region i $(1 \leqslant i \leqslant N)$, the midpoint value of ϵ is ϵ_i, ϵ ranges from $\epsilon_{i-1/2} = (\epsilon_{i-1}+\epsilon_i)/2$ to $\epsilon_{i+1/2} = (\epsilon_i+\epsilon_{i+1})/2$ and the solution is given by

$$F = A_i \exp(r_1\epsilon) + B_i \exp(r_2\epsilon). \tag{6}$$

Expanding $r_{1,2}$ for $\gamma \ll a_\epsilon/\epsilon_{\rm max}$ (i.e. $r_1 = -(kT)^{-1} + \gamma/a_\epsilon$, $r_2 = -\gamma/a_\epsilon$), the continuity conditions at the region interfaces give recursion relations for A_i and B_i,

$$B_{i+1} = B_i \frac{a_i - 2\gamma kT}{a_{i+1} - 2\gamma kT} \exp(\epsilon_{i+1/2}\gamma/\tilde{a}_i), \tag{7}$$

where $\tilde{a}_i^{-1} = a_{i+1}^{-1} - a_i^{-1}$, a_i is the value of a_ϵ at ϵ_i and

$$A_i = A_{i+1}\exp(\epsilon_{i+1/2}\gamma/\tilde{a}_i) + \left(B_{i+1}\exp(-\epsilon_{i+1/2}\gamma/\tilde{a}_i) - B_i\right) \times \exp\left(\epsilon_{i+1/2}\left[-2\gamma/a_i + (kT)^{-1}\right]\right). \tag{8}$$

$F(\epsilon=\epsilon_{\rm max})=0$ gives

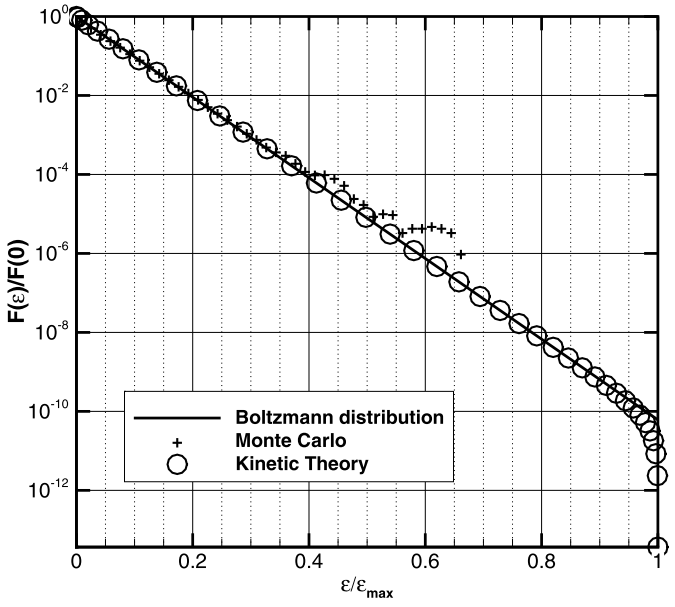

Fig. 1. $F(\epsilon)$ for a grain just before flipping near the nucleation field in Fig. 6 with $\epsilon_{\rm max}/kT \simeq 24$. Line, Boltzmann distribution f_B; +, Monte Carlo based on direct LLG calculation overlaps other results but statistical errors arise at the higher energies for which Monte Carlo can provide data; circles, MMKT, where the detailed model (shown) agrees with Eq. (15) closely enough that differences are not visible in the plot.

$$A_N = -B_N \exp\left(\epsilon_{\rm max}\left(\frac{1}{kT} - \frac{2\gamma}{a_N}\right)\right), \tag{9}$$

whereas setting $\Gamma(\epsilon=0)=0$ gives a condition on γ:

$$\gamma = \frac{a_1 B_1}{kT(B_1 - A_1)}. \tag{10}$$

Iteration of this set converges rapidly, provided $\epsilon_{\rm max} \gg kT = D_\epsilon/a$ (in practice, $N=40$ is sufficient).

When $\epsilon_{\rm max} \gg kT$, $F(\epsilon) \simeq f_B(\epsilon) \equiv f_0 \exp(-\epsilon/kT)$ and we find a simpler expression for γ. The energy flux may be written

$$\Gamma = -D_\epsilon \exp(-a_\epsilon\epsilon/D_\epsilon)\frac{\partial}{\partial\epsilon}\left(f\exp(a_\epsilon\epsilon/D_\epsilon)\right). \tag{11}$$

Conservation of probability implies

$$\frac{\partial\Gamma}{\partial\epsilon} = \gamma f, \tag{12}$$

and integrating $\frac{\partial\Gamma}{\partial\epsilon} = \gamma f_B(\epsilon)$ gives a second, approximate Γ:

$$\Gamma_{\rm approx} = \gamma f_0 kT\left(1 - \exp(-\epsilon/kT)\right). \tag{13}$$

Setting Γ in Eq. (11) equal to $\Gamma_{\rm approx}$ and integrating we obtain

$$f\exp(\epsilon/kT) - f_0 = -\gamma f_0 \int_0^\epsilon \frac{d\epsilon}{a_\epsilon}\left(\exp(\epsilon/kT) - 1\right). \tag{14}$$

If we set f equal to zero at $\epsilon_{\rm max}$, we obtain a condition which involves the two remaining terms, from which f_0 cancels and an expression for γ results. The result is

$$F \simeq f_B(\epsilon)\left(1 - \gamma/\tilde{\gamma}(\epsilon)\right), \tag{15}$$

with $\gamma = \tilde{\gamma}(\epsilon=\epsilon_{\rm max})$ and

$$\tilde{\gamma}(\epsilon) = \left[\int_0^\epsilon \frac{d\epsilon}{a_\epsilon}\left(\exp(\epsilon/kT) - 1\right)\right]^{-1}. \tag{16}$$

$F(\epsilon)$ is shown by hollow circles in Fig. 1, along with f_B and Monte Carlo results.

3. Orbit-averaged transport coefficients

This section discusses the calculation of D_ϵ and a_ϵ, as well as the barrier height and conversion of the spectrum of barrier heights to an effective mean barrier height that yields the correct mean transition rate γ. We numerically follow the orbits of the grains using the LLG equation with $\alpha = \vec{H}_{\rm th} = 0$. In this case, $\epsilon =$ constant and corresponds to a closed orbit. Conservation of energy to single precision is easily achieved using either the standard Heun or mid-point time integrators with appropriate time steps. Conservation of energy guarantees the numerical orbits close to similar accuracy. By averaging the diffusion coefficient D_ϵ and the drift a_ϵ over time, during a single orbit, we obtain D_ϵ and a_ϵ at $\epsilon = \epsilon_{\rm orbit}$.

We may find the instantaneous a_ϵ from the diffusion coefficient using the Einstein relation, (see below) or using the time derivative of the free energy,

$$\begin{aligned}\frac{dG}{dt} &= \int_\Omega \left[\frac{\delta G}{\delta \vec{M}}\cdot\frac{\partial \vec{M}}{\partial t} + \frac{\delta G}{\delta \vec{H}_{\rm a}}\cdot\frac{\partial \vec{H}_{\rm a}}{\partial t}\right] dV \\ &= \int_\Omega \left[-\vec{H}_{\rm eff}\cdot\frac{\partial \vec{M}}{\partial t} - \vec{M}\cdot\frac{\partial \vec{H}_{\rm a}}{\partial t}\right] dV \\ &= -a(\epsilon) - M_s V \vec{m}\cdot\frac{\partial \vec{H}_{\rm a}}{\partial t}, \end{aligned} \tag{17}$$

where V is the magnetic domain volume. Neglecting $\frac{\partial \vec{H}_{\rm a}}{\partial t}$ and using $\widehat{m}\cdot d\widehat{m}/dt = 0$, a_ϵ in the absence of stochastic thermal fields is

$$\begin{aligned} a_\epsilon &= M_s V \vec{H}_{\rm eff}\cdot\frac{d\widehat{m}}{dt} = M_s V \vec{H}_{\rm eff}\cdot\left(\alpha\widehat{m}\times\frac{d\widehat{m}}{dt}\right) \\ &= \alpha M_s V \vec{H}_{\rm eff}\cdot\left[-\gamma_0(\widehat{m}\cdot\vec{H}_{\rm eff})\widehat{m} + \gamma_0\vec{H}_{\rm eff} - \alpha\frac{d\widehat{m}}{dt}\right] \\ &= \frac{\alpha\gamma_0 M_s V}{1+\alpha^2}|\widehat{m}\times\vec{H}_{\rm eff}|^2. \end{aligned} \tag{18}$$

Similarly, W.F. Brown's stochastic thermal fields [9] imply a value for D_ϵ:

$$\begin{aligned} D_\epsilon &= \frac{\langle(\delta G)^2\rangle}{2\delta t} = \frac{\delta t}{2}\left\langle\left(-M_s V\vec{H}_{\rm eff}\cdot\frac{d\widehat{m}(\vec{H}_{\rm th})}{dt}\right)^2\right\rangle \\ &= \frac{\delta t}{2}\left(\frac{\gamma_0 M_s V}{1+\alpha^2}\right)^2\left\langle\left(\vec{H}_{\rm eff}\cdot\widehat{m}\times\vec{H}_{\rm th}\right.\right. \\ &\quad \left.\left. + \alpha(\widehat{m}\cdot\vec{H}_{\rm eff})(\widehat{m}\cdot\vec{H}_{\rm th}) - \alpha\vec{H}_{\rm th}\cdot\vec{H}_{\rm eff}\right)^2\right\rangle \\ &= \frac{\gamma_0\alpha M_s V kT}{1+\alpha^2}|\widehat{m}\times\vec{H}_{\rm eff}|^2, \end{aligned} \tag{19}$$

where $\langle\cdots\rangle$ is the ensemble average over the three independent components of $\vec{H}_{\rm th}$ each with variance $\sigma^2 = 2kT\alpha/\gamma_0 M_s V\delta t$. This expression is identical to that Brown finds in the drift–diffusion model, when allowance is made for the factor $\vec{H}_{\rm eff}$ which converts steps on the unit sphere into steps in energy, and for the fact that the energy diffusion is in one dimension. D_ϵ and a_ϵ obey an Einstein relation, $D_\epsilon/a_\epsilon = kT$. Brown finds the drift term from the Einstein relation, which confirms our result above for a_ϵ.

For $\epsilon \to \epsilon_{\rm max}$, the calculated orbit period $T_{\rm orbit} \to \infty$. (The maximum, or saddle point, is the critical region near to which the grain is expected to escape.) $T_{\rm orbit}$ does not truly diverge, because thermal fields cause diffusion in $\widehat{m}$. A search for $\epsilon_{\rm max}$ is done by starting orbits at an increasing angle from $\vec{M}_0$ (the local minimum energy). The first orbit that satisfies $\vec{M}_0\cdot(\widehat{m}\times d\widehat{m}/dt) \leqslant 0$ anywhere along the orbit has energy $\epsilon_{\rm max}$. In other words, this orbit is the first orbit that could relax via damping into an orientation at least partially anti-parallel to $\vec{M}_0$. A simple bisection search can easily find $\epsilon_{\rm max}$ to arbitrary precision once the launch angle corresponding to $\epsilon_{\rm max}$ is bracketed. D_ϵ and a_ϵ are found from a drift–diffusion equation at $\epsilon = \epsilon_{\rm orbit}$ allowing for diffusion along the orbit which will prevent grains from being trapped at the saddle point. In steady state, the orbital probability density $n(s)$ satisfies

$$\begin{aligned} 0 &= \frac{\partial}{\partial s}\left(D_m\frac{\partial n}{\partial s}\right) - \frac{\partial}{\partial s}\left(\left|\frac{d\widehat{m}}{dt}\right| n\right) \\ &= D_m\frac{\partial^2 n}{\partial s^2} - \frac{\partial}{\partial s}\left(\gamma_0|\widehat{m}\times\vec{H}_{\rm eff}|n\right), \end{aligned} \tag{20}$$

where s is the path coordinate, $D_m \equiv \langle\delta\widehat{m}\cdot\delta\widehat{m}\rangle/2\delta t = \alpha\gamma_0 kT/(1+\alpha^2)M_s V$ (which is independent of s) is the diffusion coefficient in $\widehat{m}$ due to stochastic thermal fields and averaging over orbits

$$\left\langle|\widehat{m}\times\vec{H}_{\rm eff}|^2\right\rangle_{\rm orbit} = \int_{\rm orbit} ds\, n(s)\left|\widehat{m}(s)\times\vec{H}_{\rm eff}(s)\right|^2 \Big/ \int_{\rm orbit} ds\, n(s). \tag{21}$$

Again, we use numerical LLG to follow the orbit and construct a finite difference equation

$$\begin{aligned} 0 &= \frac{2D_m}{s_{i+1}-s_{i-1}}\left(\frac{n(s_{i+1})-n(s_i)}{s_{i+1}-s_i} - \frac{n(s_i)-n(s_{i-1})}{s_i - s_{i-1}}\right) \\ &\quad - \gamma_0\frac{|\widehat{m}\times\vec{H}_{\rm eff}|_{i+1}n(s_{i+1}) - |\widehat{m}\times\vec{H}_{\rm eff}|_{i-1}n(s_{i-1})}{s_{i+1}-s_{i-1}}. \end{aligned} \tag{22}$$

With periodic boundary conditions we obtain a simple cyclic tridiagonal system for the density, shown in Fig. 2, and hence the appropriately averaged D_ϵ and a_ϵ, Fig. 3. Angular diffusion was included in this approach, but not diffusion of $\widehat{m}$ in energy, since diffusion in energy is handled by the kinetic equation for the probability with respect to energy.

Finally in this section we note that the motion of neighboring grains causes the barrier height to fluctuate. One of the most important uses of our expression for the transition rate γ, Eq. (16), is that it allows us to find the mean barrier height, from the distribution of barrier heights which we obtain by orbit following.

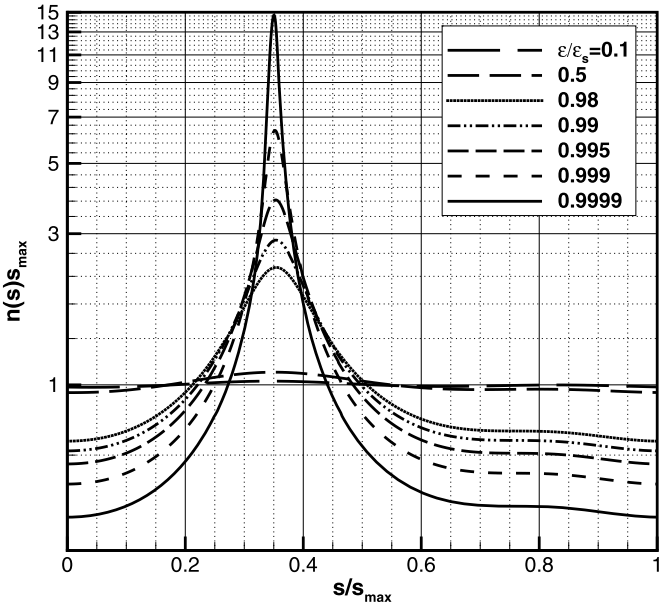

Fig. 2. Orbit probability density as a function of orbit coordinate at different energies for the same grain as in Fig. 1, normalized so that a uniform orbit density would be $1/s_{\rm max}$ and $s = 0$ is the location of the maximum $|\widehat{m}\times\vec{H}_{\rm eff}|$ in the orbit.

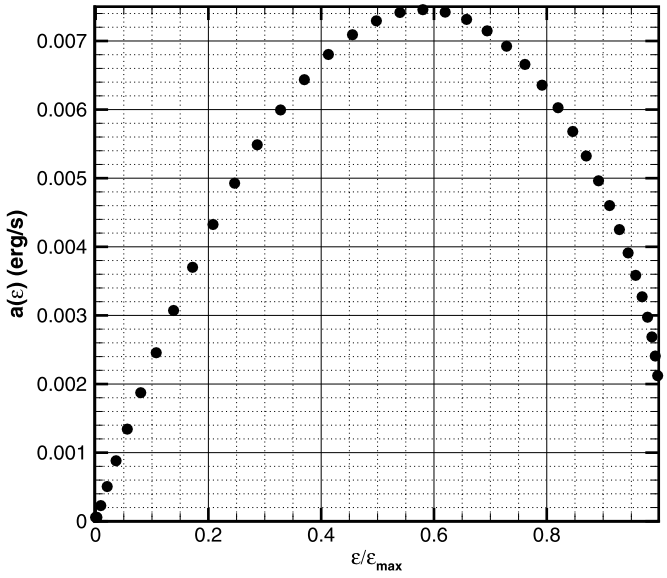

Fig. 3. a_ϵ for the same grain as in Fig. 1 computed using Eq. (21) and the orbital density as shown in Fig. 2.

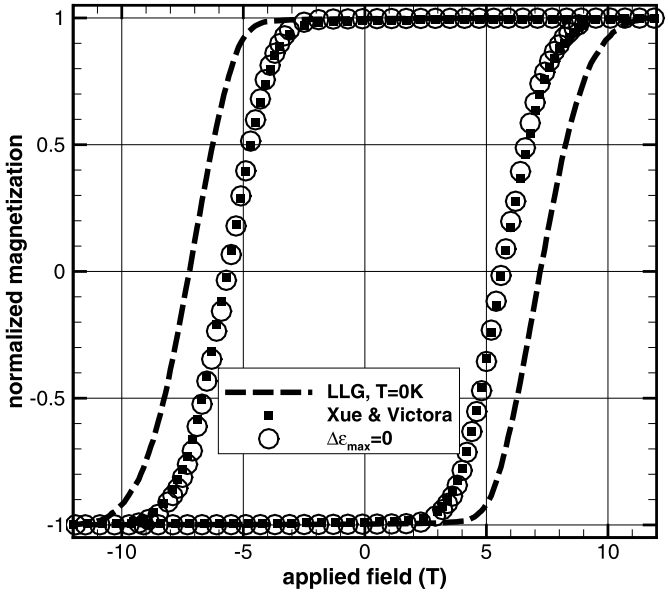

Fig. 4. Perpendicular easy axis hysteresis loop (300 K, 190 Oe/s) for a set of grains with very high energy barriers: solid squares, XV method [13]; open circles, MMKT; dash, direct LLG at $T = 0$ K overestimates coercivity, nucleation and saturation fields.

This is the subject of the remainder of this section. The fluctuation in barrier height can be summarized by a probability distribution $p_B(\epsilon_{\max})$ such that $p_B(\epsilon_{\max})\,d\epsilon_{\max}$ is the probability of the barrier having height in the range $\epsilon_{\max}$ to $\epsilon_{\max}+d\epsilon_{\max}$. The distribution of barrier heights was found by running the full micromagnetic simulation including damping and stochastic fields for 1 ns then freezing the orientations of the moments. The barrier height is then found in that configuration; this is repeated hundreds of times. Then the transition rate $\gamma(\epsilon_{\max})$ may be averaged over $p_B(\epsilon_{\max})$, to obtain $\overline{\gamma}$. We use $\overline{\gamma}$ in the expression for $\gamma(\epsilon_{\max})$ to find the effective barrier height, so $\epsilon_{\max}$ becomes $\epsilon_{\max}+\Delta\epsilon_{\max}$ where $\Delta\epsilon_{\max}<0$. In this Letter we treat $\Delta\epsilon_{\max}$ as a (different) constant for each set of grains during hysteresis. We calculated $\Delta\epsilon_{\max}$ at different points in the hysteresis loop; $\Delta\epsilon_{\max}$ was constant within statistical errors, but its potential variation is an important issue for future work.

4. Hysteresis curves

This section employs the transition rate γ to find hysteresis curves, in a conventional Monte Carlo simulation. All results presented are averages over six samples, each of at least 500 grains. The magnetization is initialized in a saturated state. We then step over external applied field values (481 uniform steps here). For each field step, $\Delta\vec{H}_a$, we must wait for a time $\Delta\vec{H}_a/(\partial\vec{H}_a/\partial t)$ before the next field step. Looping until this wait time is reached, we first allow the collection of grains to relax in the absence of stochastic thermal fields. We then freeze the magnetization orientation and find γ for each grain. The next grain to flip is selected randomly given that the probability of a grain being the first to flip is $\gamma/\sum_{\text{grain}}\gamma$. The actual time for that grain to flip is given by $-\ln\eta/\gamma$ where $\eta\in(0:1]$ is a uniformly distributed random number. If the sum of this time, plus the time elapsed at this applied field prior to updating the current grain, is less than the wait time, the grain is flipped and we loop to find the next grain that flips. Otherwise the grain does not flip and we move to the next applied field.

Compared to the Xue & Victora (XV) method [13] the micromagnetic kinetic theory (MMKT) loop takes about twice as long to perform the final loop, but reference (the most time consuming part of XV) and scaling runs are avoided, along with their artificial temperatures and sweep rates. (Unlike XV, arbitrary and changing sweep rates are allowed in MMKT, provided $\frac{\partial\vec{H}_a}{\partial t}$ in Eq. (17) remains small.)

We present three sets of hysteresis loops for periodic media with Voronoi-like grains. The first employs realistic parameters for future granular storage media in hard disk drive applications. The media consist of grains of uniform height of 7 nm with average diameter of 7.2 nm and a log-normal standard deviation of 0.17 at a volume packing fraction of 65%. The uniaxial magnetocrystalline distribution is also log-normal with a mean of 90 kOe and a standard deviation of 0.14, a Gaussian distribution in easy axis angle from the plane normal with standard deviation of 3^0 on a sphere and saturation magnetization, M_s, of 1000 emu/cc. Fig. 4 shows the predicted experimental easy axis loop at 300 K and a field sweep rate of 190 Oe/s. XV [13] results are the squares, where the "reference run" had an artificial temperature $T=3000$ K and a sweep rate (SR) of 100 Oe/ns. The "scaling run" ($T=4005$ K, $SR=10$ Oe/ns) reproduced the reference run. The XV scaling implies we should use ($T=1278$ K, $SR=10$ Oe/ns) for the final loop shown in Fig. 4. The MMKT method required only the actual physical temperature (300 K) and sweep rate (190 Oe/s). We see generally excellent agreement. The slight differences seen at both the nucleation and saturation points may be due in part to the fact that XV assumes the same attempt frequency throughout the major loop.

We next simulate the original loops in [13]. Fig. 5 shows the hysteresis for a uniformly thick granular medium of 10 nm with average grain diameter of 9.6 nm and log-normal distribution standard deviation of 0.15 at 85% volume packing fraction. The easy axes of the grains are randomly distributed in-plane with uniform magnitude of 9 kOe and $M_s=400$ emu/cc. XV was again followed using a "reference run" ($T=300$ K, $SR=5$ Oe/ns). The scaling run had ($T=425$ K, $SR=50$ Oe/ns) and according to the scaling rule the values ($T=550$ K, $SR=50$ Oe/ns) correspond to the "experimental" case with ($T=300$ K, $SR=0.5$ Oe/ns). These "experimental" values are unrealistic, but allow direct computation of the loop using LLG and stochastic fields (line in Fig. 5.) The MMKT method (circles) only required the "experimental" temperature and field sweep rate. The effect of including energy barrier

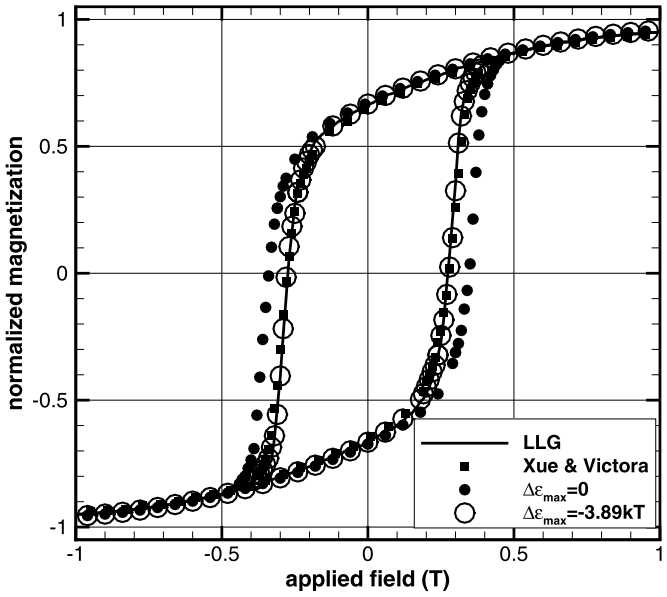

Fig. 5. In-plane hysteresis loop ($T = 300$ K, $SR = 0.5$ Oe/ns) for a set of grains with randomly orientated in-plane easy axis and low energy barriers: line, direct calculation; solid squares, XV method [13]; circles, MMKT.

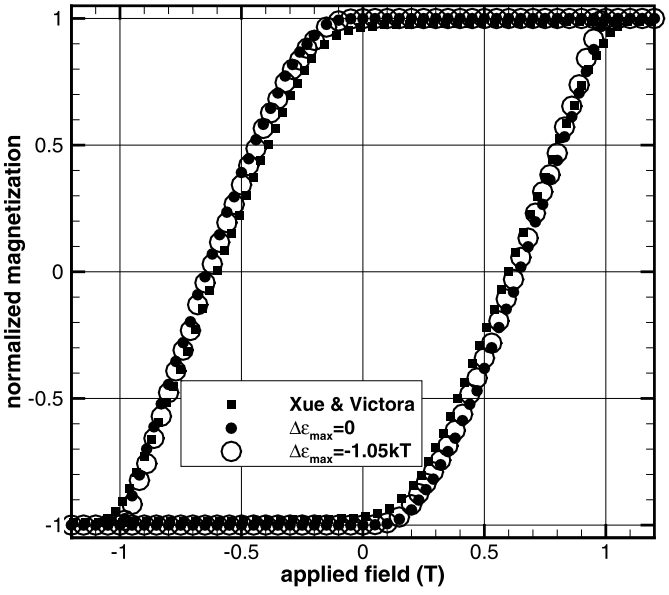

Fig. 6. Perpendicular easy axis hysteresis loop ($T = 300$ K, $SR = 50$ Oe/s) for a set of grains with moderate energy barrier heights: solid squares, XV method [13]; circles, MMKT.

lowering is shown. γ is so high here that the MMKT assumptions are marginally satisfied, but when γ is high, LLG is available instead of XV or MMKT.

The second example given in [13] is for a uniformly thick granular medium of 18 nm with average grain diameter of 12 nm and log-normal distribution standard deviation of 0.15 at 85% volume packing fraction. The easy axis is Gaussian distributed on a sphere centered about the normal with standard deviation of 1^0 with uniform magnitude of 11.4 kOe and $M_s = 350$ emu/cc. The "reference run" for XV had ($T = 300$ K, $SR = 5$ Oe/ns). The scaling run had ($T = 396$ K, $SR = 50$ Oe/ns) and according to the scaling, ($T = 550$ K, $SR = 50$ Oe/ns) were used to compute the loop corresponding to experimental values ($T = 300$ K, $SR = 50$ Oe/s). MMKT results with and without the energy barrier reduction due to the dynamics of other grains are also shown in Fig. 6.

5. Conclusion

A kinetic theory was developed to find the transition rate of a recording media grain's magnetization in a magnetic field, escaping a local energy minimum. Numerical LLG was used to find transport coefficients with respect to energy, appropriately orbit-averaged, and the height of the energy barrier which must be overcome. Difficulties with the trajectory-average near the saddle point were resolved by solving a transport equation along an orbit to include diffusion along $\epsilon = \epsilon_{\text{orbit}}$. The transport coefficients obey an Einstein relation, but they vary dramatically, being smallest at the energy minimum and the saddle point, Fig. 3.

All of the parameters of the theory are obtained by orbit following, for a small number of orbits. Monte Carlo simulations based on these rates gave $M(H)$ loops which are very close to those obtained in the standard way.

The transport model using time-averaged transport coefficients was adequate for a system with very deep energy barriers preventing individual grains from flipping. In general, however, the mean barrier height was changed by $\Delta\epsilon_{\max} < 0$ because of the precession of near-neighbor grains. For moderate or small barriers, lowering of the barrier by the magnitude of $\Delta\epsilon_{\max}$ is physically significant. The variation of $\Delta\epsilon_{\max}$ throughout the hysteresis loop is an important topic for future work.

References

[1] O.G. Heinonen, D.K. Schreiber, A.K. Petford-Long, Micromagnetic modeling of spin–wave dynamics in exchange-biased permalloy disks, Phys. Rev. B 76 (2007) 144407.
[2] A. Romeo, G. Finocchio, M. Carpentieri, L. Torres, G. Consolo, B. Azzerboni, A numerical solution of the magnetization reversal modeling in a permalloy thin film using fifth order Runge–Kutta method with adaptive step size control, Physica B 403 (2008) 464–468.
[3] Sang-Koog Kim, Micromagnetic computer simulations of spin waves in nanometre-scale patterned magnetic elements, J. Phys. D, Appl. Phys. 43 (2010) 264004.
[4] Y. Kanai, M. Saiki, K. Hirasawa, T. Tsukamomo, K. Yoshida, Landau–Lifshitz–Gilbert micromagnetic analysis of single-pole-type write head for perpendicular magnetic recording using full-fft program on pc cluster system, IEEE Trans. Magn. 44 (2008) 1602.
[5] J. Fidler, T. Schrefl, W. Scholz, D. Suess, R. Dittrich, M. Kirschner, Micromagnetic modelling – the current state of the art, J. Phys. D, Appl. Phys. 33 (2000) R135.
[6] J. Fidler, T. Schrefl, Micromagnetic modelling and magnetization processes, J. Magn. Magn. Mater. 272 (2004) 641–646.
[7] D.V. Berkov, J. Miltat, Spin-torque driven magnetization dynamics: micromagnetic modeling, J. Magn. Magn. Mater. 320 (2008) 1238–1259.
[8] Martin L. Plumer, Johannes Van Ek, Dieter Weller, The Physics of Ultra-High-Density Magnetic Recording, Springer, 2001.
[9] W.F. Brown, Thermal fluctuations of a single-domain particle, Phys. Rev. 130 (1963) 1677.
[10] W.T. Coffey, D.S.F. Crothers, J.L. Dormann, L.J. Geoghegan, Yu.P. Kalmykov, J.T. Waldron, A.W. Wickstead, Effect of an oblique magnetic field on the superparamagnetic relaxation time, Phys. Rev. B 52 (1995) 15951–15965.
[11] W. Scholtz, T. Schrefl, J. Fidler, Micromagnetic simulation of thermally activated switching in fine particles, J. Magn. Magn. Mater. 403 (2008) 296–304.
[12] J. Schratzberger, J. Lee, M. Fuger, J. Fidler, G. Fiedler, T. Schrefl, D. Suess, Validation of the transition state theory with Langevin-dynamics simulations, J. Appl. Phys. 108 (2010) 033915.
[13] Jianhua Xue, R.H. Victora, Micromagnetic predictions for thermally assisted reversal over long time scales, Appl. Phys. Lett. 77 (2000) 3432–3434.
[14] D.M. Alpakov, P.B. Visscher, Spin-torque switching: Fokker–Planck rate calculation, Phys. Rev. B 72 (2005) 180405(R).
[15] D.L. Scharfetter, H.K. Gummel, Large signal analysis of a silicon read diode oscillator, IEEE Trans. Electron Devices 16 (1969) 64–77.